Report

Current Biology

Bats use topography and nocturnal updrafts to fly high and fast

Highlights

- European free-tailed bats use uplifting winds to ascend 1,600 m above ground level
- High-elevation ascents are predicted by geography with high orographic uplift
- European free-tailed bats can fly at self-powered airspeeds over 130 kmh^{-1}
- Bats deftly exploit nocturnal energy landscapes similar to diurnal birds

Authors

M. Teague O'Mara, Francisco Amorim, Martina Scacco, ..., Pedro Beja, Hugo Rebelo, Dina K.N. Dechmann

Correspondence

teague.omara@selu.edu

In Brief

O'Mara et al. use high-resolution GPS tracking and atmospheric models to show that, similar to diurnal birds, European free-tailed bats use uplifting winds generated by the nocturnal energy landscape to rapidly ascend over 1,600 m above ground level and achieve maximum self-powered airspeeds over 130 kmh^{-1}.

O'Mara et al., 2021, Current Biology *31*, 1311–1316
March 22, 2021
https://doi.org/10.1016/j.cub.2020.12.042

CellPress

Current Biology

CellPress

Report

Bats use topography and nocturnal updrafts to fly high and fast

M. Teague O'Mara,[1,2,3,10,*] Francisco Amorim,[4,5] Martina Scacco,[2,3] Gary F. McCracken,[6] Kamran Safi,[2,3] Vanessa Mata,[4,5] Ricardo Tomé,[7] Sharon Swartz,[8] Martin Wikelski,[2,3] Pedro Beja,[4,9] Hugo Rebelo,[4,9] and Dina K.N. Dechmann[2,3]

[1]Southeastern Louisiana University, Hammond, LA, USA
[2]Max Planck Institute of Animal Behavior, Radolfzell Germany
[3]Centre for the Advanced Study of Collective Behaviour, University of Konstanz, 78457 Konstanz, Germany
[4]CIBIO-InBIO, Research Center in Biodiversity and Genetic Resources, University of Porto, Vairão, Portugal
[5]Departamento de Biologia, Faculdade de Ciências, Universidade do Porto, Porto, Portugal
[6]Department of Ecology & Evolutionary Biology, University of Tennessee, Knoxville, TN, USA
[7]Instituto Dom Luiz (IDL), Faculdade de Ciências, Universidade de Lisboa, 1749-016 Lisboa, Portugal
[8]Department of Ecology and Evolutionary Biology and School of Engineering, Brown University, Providence, RI, USA
[9]CIBIO-InBIO, Research Center in Biodiversity and Genetic Resources, Institute of Agronomy, University of Lisbon, Lisbon, Portugal
[10]Lead contact
*Correspondence: teague.omara@selu.edu
https://doi.org/10.1016/j.cub.2020.12.042

SUMMARY

During the day, flying animals exploit the environmental energy landscape by seeking out thermal or orographic uplift, or extracting energy from wind gradients.[1–6] However, most of these energy sources are not thought to be available at night because of the lower thermal potential in the nocturnal atmosphere, as well as the difficulty of locating features that generate uplift. Despite this, several bat species have been observed hundreds to thousands of meters above the ground.[7–9] Individuals make repeated, energetically costly high-altitude ascents,[10–13] and others fly at some of the fastest speeds observed for powered vertebrate flight.[14] We hypothesized that bats use orographic uplift to reach high altitudes,[9,15–17] and that both this uplift and bat high-altitude ascents would be highly predictable.[18] By superimposing detailed three-dimensional GPS tracking of European free-tailed bats (*Tadarida teniotis*) on high-resolution regional wind data, we show that bats do indeed use the energy of orographic uplift to climb to over 1,600 m, and also that they reach maximum sustained self-powered airspeeds of 135 km h^{-1}. We show that wind and topography can predict areas of the landscape able to support high-altitude ascents, and that bats use these locations to reach high altitudes while reducing airspeeds. Bats then integrate wind conditions to guide high-altitude ascents, deftly exploiting vertical wind energy in the nocturnal landscape.

RESULTS AND DISCUSSION

We fit European free-tailed bats with GPS loggers that recorded their three-dimensional location every 30 s and tracked them for 1–3 days during 5.9 ± 1.9 h per night (Table S1). Flight trajectories of eight European free-tailed bats near Santa Comba de Vilariça (41.3605° N, 7.0660° W) in northeastern Portugal revealed that bats emerged from their common roost site 47 ± 16 min (mean) after sunset and flew constantly throughout the night until returning to the roost or stopping at one of several alternative roosts 65 km from the primary roost on an east-west axis (Figure 1).

European free-tailed bats reached high altitudes during their commuting flights. Their flights typically followed the rugged terrain, but on some occasions, individuals ascended over 1,680 m above ground level (AGL) in less than 20 min (Figure 2A). We used k-means clustering on the height AGL (Figure 2B) to categorize the ascending flight segments into two classes. High-altitude ascents (n = 48) reached an average maximum height of 563.5 ± 214.1 m AGL (mean ± SD) up to maximum 1,680.1 m, and moderate ascents (n = 335) reached an average maximum height of 115.2 ± 77.9 m AGL (mean ± SD) up to maximum 333.8 m (Figure 2B). During high-altitude ascents, bats climbed faster, longer, and had a lower airspeed than moderate ascents. Bats made high-altitude ascents at vertical climb rates of 0.72 ± 0.66 m s^{-1} (range: 0.05–4.5 m s^{-1}) and moderate ascents at 0.47 ± 0.51 m s^{-1} (range: 0.01–6.34 m s^{-1}; permutation test of mean differences [5,000 iterations]: mean difference = −0.25; p = 0.002), and within-ascent variance did not differ between these categories (permutation test of mean differences [5,000 iterations]: mean difference = −8.38; p = 0.105). High-altitude ascents lasted longer (high-altitude: 5.0 ± 0.58 min, moderate: 3.7 ± 0.13 min; permutation test of mean differences [5,000 iterations]: mean difference = −63.0; p = 0.005), and three-dimensional airspeeds (hereafter airspeeds) were lower than during moderate ascents (high-altitude: 5.34 ± 4.89 m s^{-1}; moderate: 7.95 ± 6.42 m s^{-1}; permutation test of mean differences [5,000 iterations]: mean difference = 2.61; p = 0.004) (Figure 2D). When bats make high-altitude ascents, they have higher vertical climb

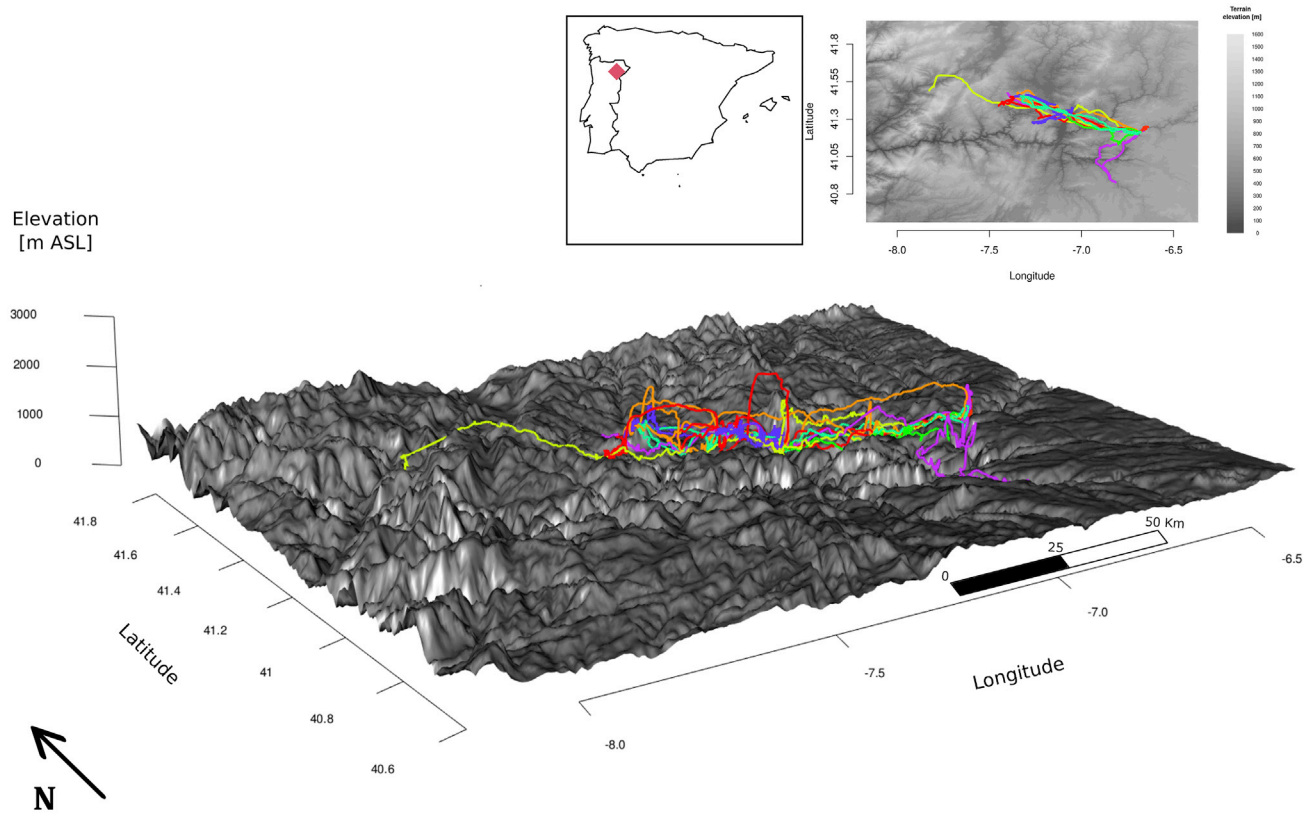

Figure 1. Tracking site and 3D flight trajectories of European free-tailed bats in northeastern Portugal

Each bat is indicated with its own color. The underlying digital elevation model (DEM) is derived from 30 m Advanced Spaceborne Thermal Emission and Reflection Radiometer) ASTER imagery and ranges from 36 m ASL to 1,411 m ASL. The insets show the capture site in relation to Portugal and Spain and also shows a top-down visualization of the study area.

See also Table S1. All data are available from the Movebank Data Repository at DOI: 10.5441/001/1.52nn82r9.

rates with lower total air speeds that are supported by orographic uplift (generalized linear mixed effects model (GLMM) with individual as a random intercept: orographic uplift: slope: 0.188 ± 0.087 SE; $X^2_1 = 10.99$; $p < 0.001$). Most bats descended quickly after reaching a peak altitude and returned to fly within 100 m AGL. Some individuals remained 350 m AGL or higher for extended periods of time (8.63 ± 12.88 min; maximum = 58.07 min) and above 1,000 m AGL for 7.68 ± 7.60 min (maximum = 19.5 min).

We then investigated the spatial distribution of high-altitude ascents versus moderate ascents to identify whether there were environmental features that produced the wind support needed to reach high altitudes and in which areas of the landscape these conditions are more likely to occur. We predicted the occurrence of high-altitude versus moderate ascents as a function of either topographic variables (elevation, slope, and aspect) or wind components (U, zonal or toward east; V, meridional or toward north; W: vertical) by using two binomial generalized additive models (Table S4). The model including wind variables captured more of the variation in the frequency of ascents than the model based on topography only (0.734 ± 0.007 versus 0.137 ± 0.002) (Table S4) and was highly accurate in predicting the occurrence of high-altitude ascents (Figures 3 and S4). Uplifting, south-easterly winds blowing across steep, south- and west-facing slopes, positively affected the probability of high-altitude ascents, whereas elevation negatively affected their probability (Figure 3A; Table S4). This indicates that nocturnal bats, like diurnal birds, use orographic lift to facilitate ascending flight and save energy.

We then used the wind and topographic models to extrapolate the predicted probability of high-altitude ascents for the entire study area by using the available topography and wind layers (the latter at 140 m AGL, averaged for the first night of tracking, 8th of August 2017). The model extrapolation was done separately for the two models and then ensembled on the basis of the accuracy of the two models (Figure 3B). The wind pattern in the study area is closely linked to the topography, and because the horizontal component of wind slows and is forced upward on the ridges, wind speeds increase on the leeward side of the ridges because of the complex terrain. Correspondingly, the ensemble prediction (area under the curve [AUC] = 0.975) shows that high-altitude ascents are more likely to occur in the valleys (low terrain elevations) as bats flew up and along windward slopes where orographic uplift would be highest and the vertical component of the wind stronger (Figure 3B). Thus, specific combinations of wind and landscape features produce enough uplift support to allow the bats to reach high altitudes, and we can use them to predict areas where high-elevation ascents are possible. The high predictability of these ascents

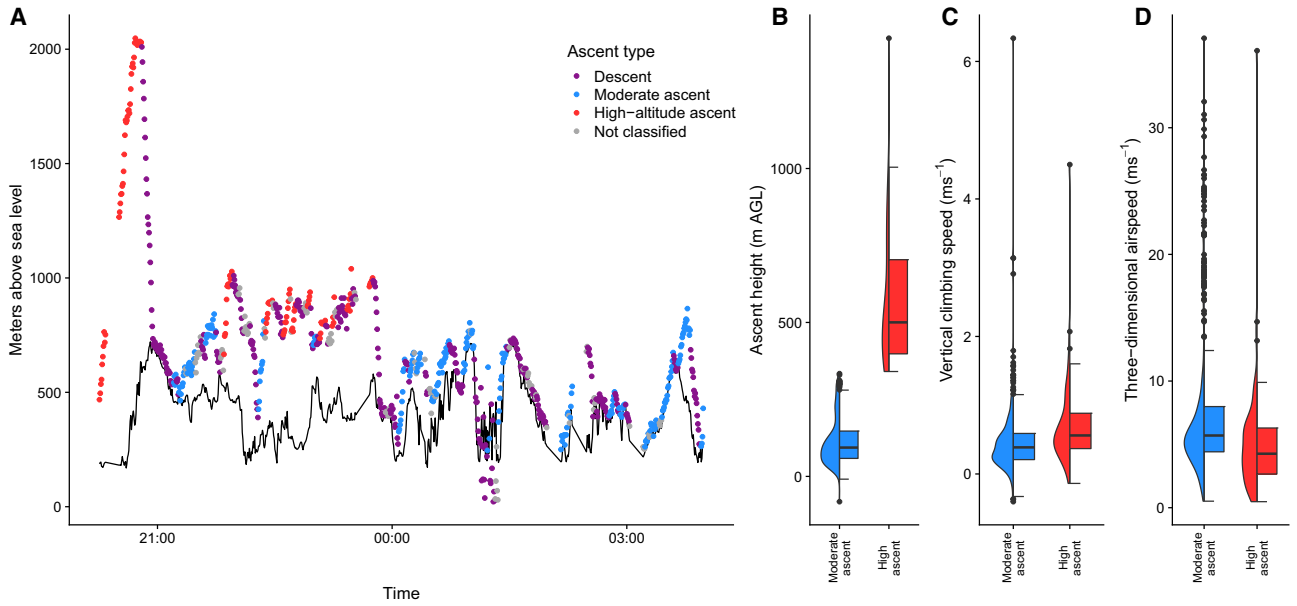

Figure 2. Bat ascent over the terrain

(A) The height profile of a portion of bat 4's flight on 2017-08-08 over the terrain (black line derived from ASTER 30 m DEM). The bat's vertical movement was clustered into segments where the bat was moving in descent, moderate ascent, high-altitude ascent, or not classified.

(B–D) Across all segments, bats in the high-altitude ascents (B) reached higher elevation above ground and gained altitude faster (C) while decreasing their overall airspeed (D).

See also Figure S3 and Tables S3 and S4.

based on environmental variables alone suggest that bats might be able to locate and use the same environmental cues to find areas of uplifting winds, or build a cognitive map of these locations.[19,20] Although exciting, the navigation and the cognitive aspects of this high-altitude flight behavior go beyond the possibility of our analyses but suggest future avenues of study.

We also were interested in quantifying flight speeds, given that Brazilian free-tailed bats (*Tadarida brasiliensis*) have been found to achieve ground speeds up to 44.5 m s^{-1} (160 km h^{-1}) for short intervals and over 20 m s^{-1} regularly, with only brief bouts of intermittent gliding.[14] Furthermore, their airspeeds, i.e., flight speed in relation to the column of moving air, are far beyond expectations for a 10–12 g animal on the basis of muscle power alone.[19,20] European free-tailed bats are 2–4 times larger (20–40 g), and should have the potential to attain even higher speeds that can be measured through high-resolution GPS tracking.[14,21] We combined the three-dimensional GPS locations with the three-dimensional wind values to calculate self-powered airspeed in three dimensions and measure how bats moved within the full space of the air column. These three-dimensional airspeeds confirmed exceptionally high flight speeds for European free-tailed bats, which had peak airspeeds of 135 km h^{-1} (37.5 ms^{-1}) and ground speeds (two-dimensional) of 149 km h^{-1} (41.2 m s^{-1}). Fifteen percent of our observations were higher than the predicted optimum speed for fast, economical, long-range movements (maximum range speed = 8.97 m s^{-1}), and flight segments with continuous airspeeds over 12 m s^{-1} lasted for 12.9 ± 10.0 min. We observed airspeeds greater than 20 m s^{-1} in segments where speeds of at least 12 m s^{-1} had been maintained for 12.7 ± 11.10 min. These fastest speeds were rare but part of a continuous distribution of high airspeeds (Figure 4). Analysis of the error distribution and location displacement shows that tag location error has its largest effects at slow speeds (Figure S3), and that the high speeds we observe occurred under ideal GPS conditions (Figure S1). In contrast, mean (± SD) airspeed over all individuals and nights was 4.68 ± 3.79, which is slightly lower than the estimated minimum power airspeed (5.54 m s^{-1}) that allows bats to minimize their flight costs, and mean ground speed was 5.63 ± 3.66 m s^{-1} (Figure 4). The lower airspeed in relation to ground speed in our data reflects positive mean tailwind support for most of the bat trajectories (1.06 ± 1.47 m s^{-1}).

We demonstrate that (1) bats reduced airspeed with increasing tailwind support, (2) increased airspeed with cross winds, and (3) tended to fly faster at higher altitudes (generalized additive mixed effects model [GAMM]) results in Table S2). The higher airspeeds we observed at higher elevations are due largely to the steep decline in wind speed at higher altitudes (e.g., Figure S3). Bats also increased airspeed slightly as they descended (GAMM height change slope: −0.002 ± 0.0002) (Table S2), but the fastest airspeeds were not observed during steep descents. Importantly, there was no effect of altitude change for flights at airspeeds greater than 15 m s^{-1} (n = 130). The fastest speeds we observed in European free-tailed bats were during level and moderately descending, not stooping, flight, and in sections of flight that appear to be commuting. It is unclear why these extreme, but rare, speeds are used by European free-tailed bats when the majority of their self-powered airspeeds are much lower. Their moth prey fly considerably slower, making foraging the unlikely cause, but their foraging and roosting areas are separated by sometimes 65 km (Figure 1). There

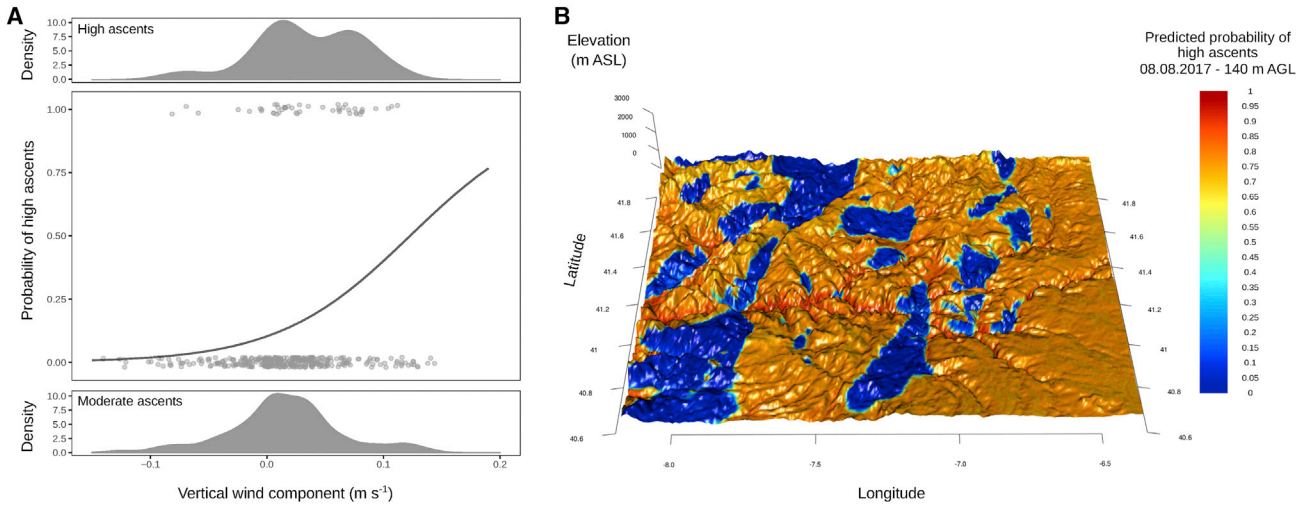

Figure 3. Probability of high-altitude ascents versus moderate ascents across the study area

(A) Probability of high-altitude ascents as predicted by the vertical component of the wind vector.

(B) Probability of high-altitude ascents across the study area, extrapolated from the ensembled predictions of wind and topographic models. The predicted probability of high ascent is not homogeneously distributed across the landscape: south- and east-facing slopes, particularly those adjacent to ravines that can funnel the localized winds blowing from the southeast into orographic uplift, have the highest probability of generating high-altitude ascents.

See also Figure S4 and Table S4.

could be substantial pressure to minimize travel time instead of travel costs, in which case high speeds would be beneficial. Additionally, the fastest speeds of common swifts (31.1 m s^{-1}) occur during mating displays.[22] This raises the possibility that the tracked bats are engaging in other behaviors beyond foraging when flying at speeds over 20 m s^{-1}, and suggests future work to understand this rare flight behavior.

We find that small differences in the underlying topography can dramatically change the aerial energy landscape even for nocturnal animals and present enormous opportunities for individuals that can exploit them.[3,6,23] The European free-tailed bat diet primarily comprises migratory moths[9] that often occur in large numbers at altitudes of 200–600 m during spring and autumn when insects accumulate in layers and exploit transport opportunities in low-level nocturnal jets.[24,25] Our study was in August during the fall migration season, and highest windspeeds and considerable activity of bats (23% of GPS locations) was observed at altitudes where aggregations of migratory moths are expected. Bats might actively exploit fine-scale updraft components to carry out otherwise costly exploratory flights in search of rich patches of migratory insects. Insects might also aggregate in eddies on the lee side of slopes where waves or rotors of descending winds concentrate migrating insects into dense patches.[26] Bats would then simply need to ride the wind currents, which would bring them directly to these eddies and rich foraging patches without the risk of extensive searching. By following the wind, bats could both lower their overall costs of flight and find dense patches of prey with low searching costs. Because migratory moths are unlikely to occur in appreciable numbers at altitudes above 1,000 m,[25–27] foraging is an unlikely explanation for the flights of bats to the highest altitudes observed. These flights might serve other purposes. For example, Egyptian fruit bats that find their food on the ground use high-altitude flights to view distant landmarks and better navigate long distances.[13]

One would expect bats to repeatedly use areas where wind conditions allow them to simultaneously minimize the costs of commutes and access higher altitudes. Most bats we observed moved along a regular route but did not appear constrained by corridors in the landscape. Because the wind generally blew toward the west and most of the higher terrain was oriented along a north-south axis, air currents provided predictable uplift that could reduce energetic cost of ascents. Non-exclusively, bats might have employed low-cost, direct paths and passively ride ascending columns of air until they descended when winds slowed, be it intentional or not (Figure S3). Environmental data at resolution similar to that of the behaviors of interest allow us to make powerful inferences into how animals use their environments. As technological advances allow tracking of body accelerations, wing motions, and muscle activation patterns,[27] the resulting insights concerning body and wing posture and power output will allow us to test this hypothesis and further reveal how these animals behave at finer scales, including within the moving air column.

The high-altitude ascents of European free-tailed bats are particularly impressive compared with those of other bat species. Free-tailed bats ascend at similar or lower speeds than bird flocks tracked by radar that can climb at rates over 1 m s^{-1} to reach migration altitudes.[28] However, European free-tailed bat tracks closely resemble those of migrating individual Swainson's thrushes that climb at 0.4 m s^{-1} in an undulating pattern.[29] Foraging mouse-tailed bats in Israel[11] and Theobald's tomb bats in Thailand[12] also employ high-altitude ascents periodically and might use energy provided by the landscape in similar ways. In contrast, the short foraging ascents of over 300 m and highly variable migration altitudes of European common noctule bats have not been explained by changing weather conditions or apparent foraging success.[10,30] Our results suggest that many bat species take advantage of fine-scale interactions of the

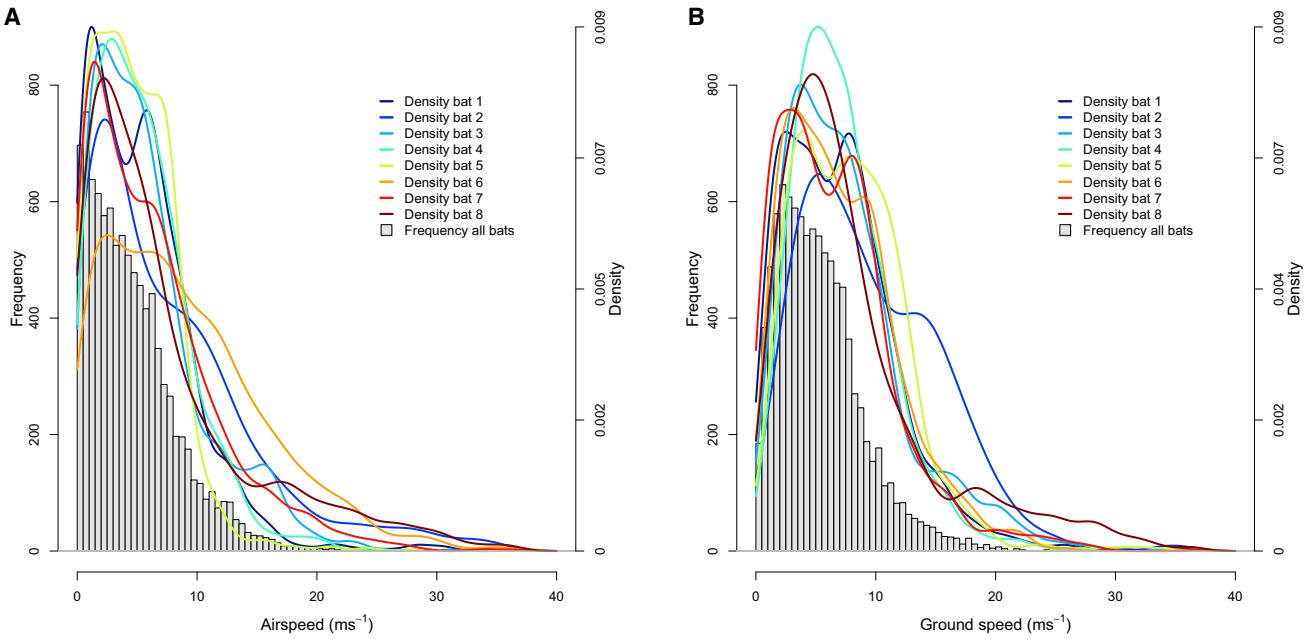

Figure 4. European free-tailed bat flight speeds

(A and B) Airspeed (A) and ground speed (B) are shown with the cumulative frequency distribution for all bats, and each individual bat's kernel density normalized to a sum of one.

See also Figures S1, S2, and S4 and Tables S1 and S2.

landscape and wind resulting in the observed roller-coaster flights. This pushes these small mammals to extraordinary heights, by using the landscape much like gulls surfing urban airflows,[6] and is an important step forward to describe how nocturnal animals move in three-dimensional space. This builds a foundation for future work investigating the mechanics not only of how bats exploit ascending columns of air efficiently, but also how they achieve these astonishing horizontal speeds. This will help to understand more generally how adaptation in bat flight, which differs dramatically from birds, has been shaped by the distinctive energy landscape of the night sky.

STAR★METHODS

Detailed methods are provided in the online version of this paper and include the following:

- KEY RESOURCES TABLE
- RESOURCE AVAILABILITY
  - Lead contact
  - Materials availability
  - Data and code availability
- EXPERIMENTAL MODEL AND SUBJECTS DETAIL
- METHOD DETAILS
  - GPS Attachment and Data Collection
  - Speed Calculations and Wind Conditions
  - Wind and Altitude Effects on Airspeed
  - Data Quality, GPS Error, and Filtering Methods
  - Predicting High-altitude Ascents
  - Environmental Predictors
  - Models for High-Altitude Ascents
  - Effect of sample size on model performance
- QUANTIFICATION AND STATISTICAL ANALYSIS

SUPPLEMENTAL INFORMATION

Supplemental Information can be found online at https://doi.org/10.1016/j.cub.2020.12.042.

ACKNOWLEDGMENTS

We thank Marion Muturi, Pedro Leote, Virgínia Duro, and volunteers from PALOMBAR for support during this project, and Jason Chapman and two anonymous reviewers for suggestions that improved the manuscript. Partial funding was provided by the Deutsche Forschungsgemeinschaft under Germany's Excellence Strategy (EXC 2117 – 42203798) to M.W., D.K.N.D., and M.T.O.; the Fundação para a Ciência e a Tecnologia, Portugal (UIDB/50019/2020 – IDL to R.T., LTER/BIA-BEC/0004/2009 to H.R., F.A., V.M., and P.R., PD/BD/52606/2014 to F.A., and IF/00497/2013 to H.R.), and the Energias de Portugal Biodiversity Chair.

AUTHOR CONTRIBUTIONS

Conceptualization: all authors; methodology: M.T.O., F.A., D.K.N.D., V.M., H.R., and G.F.M.; investigation: M.T.O., F.A., D.K.N.D., V.M., H.R., G.F.M., and R.T.; formal analysis: M.T.O., F.A., M.S., K.S., and R.T.; writing – original draft: M.T.O., M.S., and F.A; writing – final draft: all authors.

DECLARATION OF INTERESTS

Authors declare no competing interests.

Received: July 28, 2020
Revised: October 6, 2020
Accepted: December 23, 2020
Published: February 4, 2021

REFERENCES

1. Warrick, D.R., Hedrick, T.L., Biewener, A.A., Crandell, K.E., and Tobalske, B.W. (2016). Foraging at the edge of the world: low-altitude, high-speed manoeuvering in barn swallows. Philos Trans R Soc B *371*, https://doi.org/10.1098/rstb.2015.0391.
2. Wilson, R.P., Quintana, F., and Hobson, V.J. (2012). Construction of energy landscapes can clarify the movement and distribution of foraging animals. Proc. Biol. Sci. *279*, 975–980.
3. Shepard, E.L., Wilson, R.P., Rees, W.G., Grundy, E., Lambertucci, S.A., and Vosper, S.B. (2013). Energy landscapes shape animal movement ecology. Am. Nat. *182*, 298–312.
4. Péron, G., Fleming, C.H., Duriez, O., Fluhr, J., Itty, C., Lambertucci, S., Safi, K., Shepard, E.L.C., Calabrese, J.M., and Bauer, S. (2017). The energy landscape predicts flight height and wind turbine collision hazard in three species of large soaring raptor. J. Appl. Ecol. *54*, 1895–1906.
5. Duriez, O., Kato, A., Tromp, C., Dell'Omo, G., Vyssotski, A.L., Sarrazin, F., and Ropert-Coudert, Y. (2014). How cheap is soaring flight in raptors? A preliminary investigation in freely-flying vultures. PLoS ONE *9*, e84887.
6. Shepard, E.L., Williamson, C., and Windsor, S.P. (2016). Fine-scale flight strategies of gulls in urban airflows indicate risk and reward in city living. Philos Trans R Soc B *371*, https://doi.org/10.1098/rstb.2015.0394.
7. McCracken, G.F., Gillam, E.H., Westbrook, J.K., Lee, Y.F., Jensen, M.L., and Balsley, B.B. (2008). Brazilian free-tailed bats (*Tadarida brasiliensis*: Molossidae, Chiroptera) at high altitude: links to migratory insect populations. Integr. Comp. Biol. *48*, 107–118.
8. Williams, T.C., Ireland, L.C., and Williams, J.M. (1973). High altitude flights of the free-tailed bat, *Tadarida brasiliensis*, observed with radar. J. Mammal. *54*, 807–821.
9. Mata, V.A., Amorim, F., Corley, M.F., McCracken, G.F., Rebelo, H., and Beja, P. (2016). Female dietary bias towards large migratory moths in the European free-tailed bat (*Tadarida teniotis*). Biol. Lett. *12*, 20150988.
10. O'Mara, M.T., Wikelski, M., Kranstauber, B., and Dechmann, D.K.N. (2019). Common noctules exploit low levels of the aerosphere. R. Soc. Open Sci. *6*, 181942.
11. Cvikel, N., Egert Berg, K., Levin, E., Hurme, E., Borissov, I., Boonman, A., Amichai, E., and Yovel, Y. (2015). Bats aggregate to improve prey search but might be impaired when their density becomes too high. Curr. Biol. *25*, 206–211.
12. Roeleke, M., Bumrungsri, S., and Voigt, C.C. (2018). Bats probe the aerosphere during landscape-guided altitudinal flights. Mammal Rev. *48*, 7–11.
13. Tsoar, A., Nathan, R., Bartan, Y., Vyssotski, A., Dell'Omo, G., and Ulanovsky, N. (2011). Large-scale navigational map in a mammal. Proc. Natl. Acad. Sci. USA *108*, E718–E724.
14. McCracken, G.F., Safi, K., Kunz, T.H., Dechmann, D.K.N., Swartz, S.M., and Wikelski, M. (2016). Airplane tracking documents the fastest flight speeds recorded for bats. R. Soc. Open Sci. *3*, 160398.
15. Alerstam, T., Chapman, J.W., Bäckman, J., Smith, A.D., Karlsson, H., Nilsson, C., Reynolds, D.R., Klaassen, R.H., and Hill, J.K. (2011). Convergent patterns of long-distance nocturnal migration in noctuid moths and passerine birds. Proc. Biol. Sci. *278*, 3074–3080.
16. Chapman, J.W., Nilsson, C., Lim, K.S., Bäckman, J., Reynolds, D.R., and Alerstam, T. (2016). Adaptive strategies in nocturnally migrating insects and songbirds: contrasting responses to wind. J. Anim. Ecol. *85*, 115–124.
17. Chapman, J.W., Reynolds, D.R., Mouritsen, H., Hill, J.K., Riley, J.R., Sivell, D., Smith, A.D., and Woiwod, I.P. (2008). Wind selection and drift compensation optimize migratory pathways in a high-flying moth. Curr. Biol. *18*, 514–518.
18. Bohrer, G., Brandes, D., Mandel, J.T., Bildstein, K.L., Miller, T.A., Lanzone, M., Katzner, T., Maisonneuve, C., and Tremblay, J.A. (2012). Estimating updraft velocity components over large spatial scales: contrasting migration strategies of golden eagles and turkey vultures. Ecol. Lett. *15*, 96–103.
19. Harten, L., Katz, A., Goldshtein, A., Handel, M., and Yovel, Y. (2020). The ontogeny of a mammalian cognitive map in the real world. Science *369*, 194–197.
20. Toledo, S., Shohami, D., Schiffner, I., Lourie, E., Orchan, Y., Bartan, Y., and Nathan, R. (2020). Cognitive map-based navigation in wild bats revealed by a new high-throughput tracking system. Science *369*, 188–193.
21. Alerstam, T., Rosén, M., Bäckman, J., Ericson, P.G., and Hellgren, O. (2007). Flight speeds among bird species: allometric and phylogenetic effects. PLoS Biol. *5*, e197.
22. Henningsson, P., Johansson, L.C., and Hedenström, A. (2010). How swift are swifts *Apus apus?* J. Avian Biol. *41*, 94–98.
23. Rosén, M., and Hedenström, A. (2002). Soaring flight in the Eleonora's falcon (*Falco eleonorae*). Auk *119*, 835–840.
24. Drake, V.A., and Farrow, R.A. (1988). The influence of atmospheric structure and motions on insect migration. Annu. Rev. Entomol. *33*, 183–210.
25. Hu, G., Lim, K.S., Horvitz, N., Clark, S.J., Reynolds, D.R., Sapir, N., and Chapman, J.W. (2016). Mass seasonal bioflows of high-flying insect migrants. Science *354*, 1584–1587.
26. Pedgley, D.E. (1997). Concentration of flying insects by the wind. Philos Trans R Soc B *328*, 631–653.
27. Hubel, T.Y., Hristov, N.I., Swartz, S.M., and Breuer, K.S. (2012). Changes in kinematics and aerodynamics over a range of speeds in Tadarida brasiliensis, the Brazilian free-tailed bat. J. R. Soc. Interface *9*, 1120–1130.
28. Hedenström, A., and Alerstam, T. (1992). Climbing performance of migrating birds as a basis for estimating limits for fuel-carrying capacity and muscle work. J. Exp. Biol. *164*, 19–38.
29. Bowlin, M.S., Enstrom, D.A., Murphy, B.J., Plaza, E., Jurich, P., and Cochran, J. (2015). Unexplained altitude changes in a migrating thrush: Long-flight altitude data from radio-telemetry. Auk *132*, 808–816.
30. Teague O'Mara, M., Wikelski, M., Kranstauber, B., and Dechmann, D.K.N. (2019). First three-dimensional tracks of bat migration reveal large amounts of individual behavioral flexibility. Ecology *100*, e02762.
31. O'Mara, M.T., Wikelski, M., and Dechmann, D.K.N. (2014). 50 years of bat tracking: device attachment and future directions. Methods Ecol. Evol. *5*, 311–319.
32. Pennycuick, C.J. (2008). Modelling the flying bird*Volume 5* (London: Academic Press).
33. Al-Yahyai, S., Charabi, Y., and Gastli, A. (2010). Review of the use of Numerical Weather Prediction (NWP) Models for wind energy assessment. Renew. Sustain. Energy Rev. *14*, 3192–3198.
34. Skamarock, C.W., Klemp, J.B., Dudhia, J., Gill, D., Barker, D., Dudam, M., Huang, X.-Y., Wang, W., and Powers, J. (2008). A Description of the Advanced Research WRF Version 3 (Boulder: NCAR), p. 101.
35. Dee, D.P., Uppala, S.M., Simmons, A.J., Berrisford, P., Poli, P., Kobayashi, S., Andrae, U., Balmaseda, M.A., Balsamo, G., Bauer, P., et al. (2011). The ERA-Interim reanalysis: configuration and performance of the data assimilation system. Q. J. R. Meteorol. Soc. *137*, 553–597.
36. Safi, K., Kranstauber, B., Weinzierl, R., Griffin, L., Rees, E.C., Cabot, D., Cruz, S., Proaño, C., Takekawa, J.Y., Newman, S.H., et al. (2013). Flying with the wind: scale dependency of speed and direction measurements in modelling wind support in avian flight. Mov. Ecol. *1*, 4.
37. Wood, S.N. (2017). Generalized Additive Models: an Introduction with R, Second Edition (New York: Chapman and Hall).
38. Ranacher, P., Brunauer, R., Trutschnig, W., Van der Spek, S., and Reich, S. (2016). Why GPS makes distances bigger than they are. Int. J. Geogr. Inf. Sci. *30*, 316–333.

STAR★METHODS

KEY RESOURCES TABLE

REAGENT or RESOURCE	SOURCE	IDENTIFIER
Deposited Data		
Annotated GPS locations	This study	10.5441/001/1.52nn82r9
Experimental Models: Organisms/Strains		
Tadarida teniotis	Northeastern Portugal	Taxonomy ID: 59483
Software and Algorithms		
R	The R Project for Statistical Computing	https://cran.r-project.org/mirrors.html
Other		
GPS – Gipsy5	Technosmart Europe srl	https://technosmart.eu
Weather Data	European Centre for Medium-Range Weather Forecasts	https://ecmwf.int

RESOURCE AVAILABILITY

Lead contact

Further information and requests for resources should be directed to and will be fulfilled by the Lead Contact, Teague O'Mara (teague.omara@selu.edu).

Materials availability

This study did not generate new unique reagents.

Data and code availability

The datasets used generated in this study are available at the Movebank Data Repository (DOI 10.5441/001/1.52nn82r9). R code used in analysis is available from the Lead Contact. Raw GPS, environmentally annotated data, and three-dimensional interactive versions of Figure 1 and Figure S1 are available at the Movebank Data Repository (DOI 10.5441/001/1.52nn82r9).

EXPERIMENTAL MODEL AND SUBJECTS DETAIL

European free-tailed bats (*Tadarida teniotis*) were captured at evening emergence using mist nets set at the roost exits near Santa Comba de Vilariça (41.36° N, 7.07° W) in northeastern Portugal. All methods were approved by ICNF - Instituto de Conservação da Natureza e Florestas, Portugal (665/2017/CAPT).

METHOD DETAILS

GPS Attachment and Data Collection

We fit 33 lactating females (33.92 ± 1.63 g) with Gipsy5 GPS tags (Technosmart Europe srl) that were encased in a balloon. GPS tags were deployed either on collars[31] or glued to the bat's back by applying Permatype surgical cement directly to the fur and to the balloon (Table S1). Total tag weight (3.59 ± 0.21 g) was 10.59% ± 0.49% of body mass. The GPS tags had minimal measurable effects on bat body condition (body mass / forearm length). Tagged bats generally maintained or improved their body condition (mean ± SD of the change in individual body condition: 0.135 ± 0.374, range = −0.036 – 0.072, permutation test of mean differences (5,000 iterations:[10] mean difference = 0.0175, p = 0.108). Overall, the body condition of bats that wore a GPS tag, both before and after tagging, was higher than for bats that did not receive a GPS tag and were captured on the same night ($F_{2, 236} = 40.47$, $p < 0.001$). Tags were either recovered by recapturing bats at the same location or locating the tags on the ground under the roost. Based on the mean weight of our tagged bats and mean wingspan from bats from a different study that were photographed on graph paper with a fully outstretched wing (370 mm, Amorim, unpublished data), we calculated a mean power curve[32] for an unladen *T. teniotis*, and estimated a minimum power speed (V_{mp}) of 5.54 m s^{-1} and maximum range speed (V_{mr}) of 8.97 m s^{-1}.

GPS tags were programmed to record one location (latitude, longitude, height above sea level) every 30 s. We recovered 11 tags, of which 8 had recorded data for 1–3 nights and a total of 10,336 GPS locations (Table S1). We took a conservative approach to obtain the highest quality and most reliable dataset possible. We removed by hand, points that were obviously error in the tracks due to unreasonably large displacement (N = 45) and limited the dataset to consecutive points with a 20–40 s time lag. This reduced the dataset from the full 10,336 points to 9873 (3.4% loss) to yield a dataset with high temporal and spatial resolution with a regular

sampling regime. All data, including those marked as outliers and removed from analysis, and a fully annotated dataset, are available at the Movebank data repository (DOI 10.5441/001/1.52nn82r9).

Speed Calculations and Wind Conditions

We calculated segment speed as the speed between two consecutive points in three dimensions (analogous to ground speed). We then calculated three-dimensional self-powered airspeed (hereafter airspeed) from these segments by first calculating wind support based on wind data derived from a numerical weather prediction (NWP) model. NWP models can provide valuable weather forecasts at regional scales and are commonly used to describe and forecast atmospheric motions. These models can provide long time series of atmospheric data, like wind speed and direction, with very high resolution both horizontally and vertically in a given study region in a short period of time.[33] We use the high-resolution numerical weather model Weather Research and Forecasting (WRF).[34] The WRF is a next generation mesoscale forecast and assimilation system that has advanced both the understanding and prediction of mesoscale systems. It is designed for a wide range of applications, from research to operational forecasting, with a priority emphasis on horizontal resolutions below 10 km. Here the WRF model was used in hindcast mode with initial and boundary conditions provided by the ECMWF ERA-Interim Reanalysis.[35] The model used a 4 nested grid setup, with the highest horizontal resolution of 1 km and the simulation spans from August 8th to August 17th 2017, with output every 5 min.

The wind conditions at our study site were highly variable among tracking nights and elevation. The WRF model provided regional weather information at 1 km resolution every 5 min and at 68 terrain—following levels that range from the ground to nearly 20,000 m AGL. For this study, we chose 23 levels to encompass bat flight with a maximum of 2,156 m AGL. The weather variables provided by the WRF model included temperature, air pressure, and three components of the wind vector (U: zonal or toward east, V: meridional or toward north, W: vertical). We used U, V and W wind components to derive time-weighted three-dimensional wind support, which is the length of the wind vector at the location of the bat in the bat's travel direction toward the next location. Positive wind support values represent tailwind and negative values headwind. Cross wind is the length of the wind vector perpendicular to the bat's direction of travel irrespective of the side and was expressed as absolute value. We calculated the airspeed of the bat (segment speed relative to air) following,[36] adjusting the method to incorporate wind support in three dimensions and the absolute value of cross wind.

Wind and Altitude Effects on Airspeed

Bat airspeeds are likely dependent on wind support and the direction of flight. Bats should decrease their airspeed with increasing wind support, and it is possible that speeds increase with descending flights. We used generalized additive mixed effect models (R package *mgcv*[37]) to test how airspeed responds to wind support, the absolute value of crosswinds, and height above ground (Table S2). Smoothing terms of time in seconds since the first observation of the night and geographic location were included to account for spatial and temporal autocorrelation, and individual bat ID and date were included as random intercepts. Airspeed +1 was transformed on the natural log and the model fitted using a Gaussian error distribution. The best fit model (lowest AICc) included all terms (Table S2).

Data Quality, GPS Error, and Filtering Methods

There are several sources of error that could influence GPS position data and the resulting ground speed and airspeed calculation. First, location error can influence the recorded position of the data and subsequent ground speeds. This is most likely due to poor satellite coverage (number of satellites) and weak signal strength or satellite configurations that can alter the distribution of error around a location, the horizontal dilution of precision (hdop). Hdop reflects the ratio of error distribution across a major and minor axis. When the error is evenly distributed, hdop = 1, and increasing hdop values indicate an increase in the unreliability of the error probability distribution around a recorded GPS location. If this influences the likelihood of speed errors, then one would expect faster speeds to occur in more error-prone regions of satellite coverage. However, we tended to see faster ground speeds at lower hdop values (Figure S1A), and at mid-range satellite counts (Figure S1B). As expected, GPS hdop and the number of satellites used to calculate a location were negatively correlated, which indicates an increase in the quality of fixes with more satellites used.

We sought to only include the highest quality GPS positions possible. To test if there was speed-dependent difference in location error in the GPS, we first established the distribution of location error and the horizontal dilution of position (hdop) measured by the GPS using four stationary tags under open sky that recorded locations every 30 s for 3 h (Figure S2). We then used a bootstrapping procedure that shifted each observed three-dimensional GPS position in a random direction by a random distance drawn from the 95% confidence interval of the observed horizontal error (14.22 ± 12.05) and vertical error (20.86 ± 21.79 m) at each hdop value, binned to the nearest integer. Speed was then re-calculated for each segment and the process repeated 1000 times. Our randomization showed that the addition of error derived from stationary tags to our locations had the largest effect at low flight speeds, with changes in the calculated speed of approximately 1–1.5 m s^{-1} in the most extreme cases (Figures S2B–S2D). We are confident that this is a conservative estimate of location error as stationary devices will overestimate location error due to the increased precision of GPS with increasing speed.[38] Fast (or slow) speeds are then not a consequence of three-dimensional position measurement error.

The sampling interval between successive GPS locations can also influence error through an over-estimate of distance traveled when sampling frequencies are sufficiently coarse due to a decrease in spatial and temporal autocorrelation.[38] At sampling frequencies of 150 s, the overestimation of distance tends to converge at 1.5 m (a speed change of 0.01 m s^{-1}), and with sampling frequencies close to 0 s, the overestimation of distance is approximately 0.25 m.[38] This should result in the largest distances covered or fastest speeds at the slowest sampling rates. When we examined our data for a speed-sampling interval relationship, we did not see

this pattern, as the fastest ground speeds were not at longer sampling intervals but tended to be found near the mean sampling interval of 30 s (Figure S1D).

Second, the wind data could be a source of error. Airspeeds are calculated as the sum of ground speed and wind support (positive and negative). If the interpolated wind speed is incorrect, then our speed calculations would also be erroneous. The WRF model provided wind information at 1 km resolution every 5 min. There could then be spatial and temporal mismatch between locations sampled every 20–40 s and the interpolated wind values that obscures the magnitude and direction of the wind, particularly if wind gusts are present. If this has a substantial effect on airspeeds, then we would expect that periods with high wind gusts to be associated with high speeds. Likewise, if there are unmeasured tailwind effects that result from interactions between the wind and topography at small scales, then we would expect that rougher terrain, with more opportunity for localized wind changes, to be associated with high speeds. We calculated the terrain ruggedness index from the 30 m DEM to compare the relative elevation of each location to the surrounding pixels. We did not find a relationship between airspeed and the terrain ruggedness index or the speed of wind gusts (Figure S1F). The fastest airspeeds were generally found during periods with low wind gusts and at relatively flat locations with a low terrain ruggedness index.

Predicting High-altitude Ascents

Bats typically flew following the rugged terrain of our study area, but occasionally they ascended to over 1,680 m AGL (Figures 2 and S3). In this part of the analysis we (1) identified the occurrence of these events, (2) investigated if the bats can take advantage of the energy available in the landscape to perform these high-altitude flights and ultimately (3) predicted their probability of occurrence across the study area.

We characterized the altitudinal behavior of the bats in two steps. First, we applied a simple threshold to the vertical speed to separate ascending (vertical speed > 0 m s^{-1}) versus descending (vertical speed ≤ 0 m s^{-1}) segments. For the second phase we only considered ascending segments and we applied a k-means clustering algorithm with 2 clusters ($k = 2$) to the variable ''height above ground'' based on inspecting the distribution of the heights achieved during each ascent. This would then cluster ascending flights into high-altitude ascents or more typical ascents (moderate ascents). We then inspected the accuracy of the behavioral segmentation using two and three-dimensional plots (Figures 1 and S3), and tested higher number of clusters. Three clusters fit the data marginally better, but only by subdividing the moderate ascents into two groups; therefore, we chose to use $k = 2$ as a more conservative estimate. High-altitude ascents were characterized by an average maximum height 563.5 ± 214.1 m AGL (mean ± SD) up to a maximum 1,680.1 m, whereas moderate ascents reached an average maximum height of 115.2 ± 77.9 m AGL (mean ± SD) up to a maximum 333.8 m.

Environmental Predictors

We used both static and dynamic predictors to describe the environment experienced by the bats in the study area. The static predictors included variables describing the topography of the region; the terrain elevation was extracted from the digital elevation model EU-DEM 2013, with 30 m spatial granularity. We then used the DEM to compute slope and aspect (direction faced by the slope, in degrees from North). The dynamic predictors included three wind components (U, V and W) provided by the WRF model. To annotate the GPS locations with each environmental information we first performed a bilinear interpolation considering the two closest points in time. In the second step, we calculated the weighted mean of the environmental components considering both the closest values in time and height.

Models for High-Altitude Ascents

We used binomial generalized additive models (GAMs) to determine if specific environmental conditions would favor the occurrence of high-altitude ascents versus moderate ascents. We limited the model dataset to nights in which more than one individual was tracked (8^{th}–9^{th} August 2017) and we only considered ascending segments with a duration of at least 90 s (about 3 fixes). Each behavioral segment was assigned a unique ID. Two segments were considered as two different behavioral units when separated by > 60 s (about 2 fixes). We calculated the mean of each environmental predictor's values along each segment, and we considered the centroid of the segment (mean latitude and longitude) as the location of occurrence of the segment. The final dataset contained 48 high ascent segments and 335 moderate ascent segments, distributed across two nights and seven individuals (Table S3).

The environmental predictors were divided in two groups: topographic variables and wind variables. Topographic variables included terrain elevation from the DEM, slope and aspect. Wind variables included U (zonal, toward east), V (meridional, toward north), and W (vertical) component of the wind. We used these two groups of predictors to run two different models, one only based on wind and one only based on topography, to separately evaluate the effect of the two groups of predictors. W, DEM and slope were included in the models as parametric predictors, whereas U and V components were included together as a thin plate regression spline smooth term, given their nonlinear relationship with the response variable. Aspect is a circular variable and was included as cyclic cubic regression spline smooth term.

To validate the models, we used a leave-one-out cross validation approach: each model was run as many times as the number of observations in the dataset (383 times in the specific case). At each run, the model was trained with all but one observation and was used to predict the excluded observation. Therefore, at the end of the procedure we obtained a predicted vector of probability of high ascent with 383 observations (same length as the complete dataset), where each observation was predicted by the model from which this observation was excluded. Excluding one observation at a time allowed us to calculate the accuracy of the models, in terms of

area under the curve (AUC), without drastically reducing the already small sample size in the training set (as required by other cross validation approaches). The deviance explained by the two models was averaged across the 383 runs, whose consistency should reflect the absence of strong outliers among the observations. Inferences were drawn from the complete wind and topographic models (including all observations), whose results are shown in Table S4.

The weather model, including U, V, and W, explained 0.734 ± 0.007 (mean ± SD) of the deviance, with probability of high-altitude ascents significantly increased by uplifting (high W values) and southeasterly winds (positive V and negative U values). The topographic model, explained 0.137 ± 0.002 of the deviance. All variables significantly contributed to the prediction; south and west facing slopes positively affected the probability of high-altitude ascents (Figure S4). Among the parametric coefficients, elevation negatively affected the probability of high ascents, whereas slope had a positive effect (Table S4). Both the wind and the topographic models performed really well in predicting the test dataset, with an AUC of 0.955 for the wind model and of 0.728 for the topographic model (Figure S4).

Lastly, we used the complete models to extrapolate the predicted probability of high-altitude ascents across the study area, using the topographic layers and the wind layers available for the region. To simplify the predictions based on dynamic predictors (weather model), the wind layers refer to the first night of tracking (8th of August 2017) at vertical level 5, corresponding to 140 m above ground (close to the mean flight altitude of the bats). The U, V and W values available for the night were averaged. The predictions of the wind and the topographic models were ensembled: each model was assigned a weight based on their accuracy in predicting the test dataset (AUC), and the values predicted by each model were multiplied by its weight and then added to each other to obtain a final ensembled prediction (Figure 4). The ensembled prediction showed the highest accuracy in predicting the test dataset (AUC = 0.975).

Effect of sample size on model performance

The dataset used in the complete models, from which inferences were drawn, contained 335 moderate ascents and 48 high ascents and was therefore unbalanced toward moderate ascents. Here we tested if the uneven sample size of the two types of ascents had an effect on the output and interpretation of the wind and topographic models. We ran the same two models 50 times, each time including all high-altitude ascents (48 observations) and randomly sub-sampling an equal number of moderate ascents, resulting in a total of 96 observations at each run of the models. The average output of the 100 models, 50 wind models and 50 topographic models, is comparable to the results obtained from the complete models in terms of estimates of the parametric coefficients, effective degrees of freedom of the smooth terms and deviance explained.

QUANTIFICATION AND STATISTICAL ANALYSIS

All statistical tests were conducted using R 4.0.2 unless otherwise noted. K-means clustering was used to identify high or moderate ascents, and a permutation test of mean differences (5,000 iterations) was used to examine differences in ascent rates, speeds, and wind support. Binomial generalized additive models (GAMs) were used to determine if specific environmental conditions would favor the occurrence of high-altitude ascents versus moderate ascents. Generalized additive mixed effects models (GAMMS) evaluated contributing factors to bat airspeeds and included smoothing terms of time in seconds since the first observation of the night and geographic location, individual bat ID and date were included as random intercepts.